

*ARMY RESEARCH LABORATORY*



## **Black Silicon Germanium (SiGe) for Extended Wavelength Near Infrared Electro-optical Applications**

**by Fred Semendy, Patrick Taylor,  
Gregory Meissner, and Priyalal Wijewarnasuriya**

**ARL-TR-5202**

**May 2010**

## **NOTICES**

### **Disclaimers**

The findings in this report are not to be construed as an official Department of the Army position unless so designated by other authorized documents.

Citation of manufacturer's or trade names does not constitute an official endorsement or approval of the use thereof.

Destroy this report when it is no longer needed. Do not return it to the originator.

# **Army Research Laboratory**

Adelphi, MD 20783-1197

---

**ARL-TR-5202**

**May 2010**

---

## **Black Silicon Germanium (SiGe) for Extended Wavelength Near Infrared Electro-optical Applications**

**Fred Semendy, Patrick Taylor,  
Gregory Meissner, and Priyalal Wijewarnasuriya  
Sensors and Electron Devices Directorate, ARL**

<b>REPORT DOCUMENTATION PAGE</b>				<b>Form Approved OMB No. 0704-0188</b>
<p>Public reporting burden for this collection of information is estimated to average 1 hour per response, including the time for reviewing instructions, searching existing data sources, gathering and maintaining the data needed, and completing and reviewing the collection information. Send comments regarding this burden estimate or any other aspect of this collection of information, including suggestions for reducing the burden, to Department of Defense, Washington Headquarters Services, Directorate for Information Operations and Reports (0704-0188), 1215 Jefferson Davis Highway, Suite 1204, Arlington, VA 22202-4302. Respondents should be aware that notwithstanding any other provision of law, no person shall be subject to any penalty for failing to comply with a collection of information if it does not display a currently valid OMB control number.</p> <p><b>PLEASE DO NOT RETURN YOUR FORM TO THE ABOVE ADDRESS.</b></p>				
<b>1. REPORT DATE (DD-MM-YYYY)</b> May 2010	<b>2. REPORT TYPE</b> Final	<b>3. DATES COVERED (From - To)</b>		
<b>4. TITLE AND SUBTITLE</b> Black Silicon Germanium (SiGe) for Extended Wavelength Near Infrared Electro-optical Applications			<b>5a. CONTRACT NUMBER</b>	
			<b>5b. GRANT NUMBER</b>	
			<b>5c. PROGRAM ELEMENT NUMBER</b>	
<b>6. AUTHOR(S)</b> Fred Semenyd, Patrick Taylor, Gregory Meissner, and Priyalal Wijewarnasuriya			<b>5d. PROJECT NUMBER</b>	
			<b>5e. TASK NUMBER</b>	
			<b>5f. WORK UNIT NUMBER</b>	
<b>7. PERFORMING ORGANIZATION NAME(S) AND ADDRESS(ES)</b> U.S. Army Research Laboratory ATTN: RDRL-SEE-I 2800 Powder Mill Road Adelphi, MD 20783-1197			<b>8. PERFORMING ORGANIZATION REPORT NUMBER</b>	ARL-TR-5202
<b>9. SPONSORING/MONITORING AGENCY NAME(S) AND ADDRESS(ES)</b>			<b>10. SPONSOR/MONITOR'S ACRONYM(S)</b>	
			<b>11. SPONSOR/MONITOR'S REPORT NUMBER(S)</b>	
<b>12. DISTRIBUTION/AVAILABILITY STATEMENT</b> Approved for public release; distribution unlimited.				
<b>13. SUPPLEMENTARY NOTES</b>				
<b>14. ABSTRACT</b> We have investigated for the first time the reflectivity and absorbance of black silicon-germanium ( $\text{Si}_{1-x}\text{Ge}_x$ ). Black $\text{Si}_{1-x}\text{Ge}_x$ was produced by metal enhanced chemical etching using nanometer-scale gold particles as catalyst and HF:H <sub>2</sub> O <sub>2</sub> :CH <sub>3</sub> COOH etchant. The etched surface was black, textured, and showed strong suppression of reflectivity and enhancement of absorption in the near-infrared region. These properties are consistent with $\text{Si}_{1-x}\text{Ge}_x$ becoming highly micro-structured due to metal catalysis and wet etching. The lowering of reflection and enhancement of absorption in $\text{Si}_{1-x}\text{Ge}_x$ is an important milestone towards practical, extended wavelength (~2 $\mu\text{m}$ ) electro-optical applications.				
<b>15. SUBJECT TERMS</b> SiGe, Black, texturing, optical properties, infrared, compositional				
<b>16. SECURITY CLASSIFICATION OF:</b>		<b>17. LIMITATION OF ABSTRACT</b>	<b>18. NUMBER OF PAGES</b>	<b>19a. NAME OF RESPONSIBLE PERSON</b>
a. REPORT Unclassified	b. ABSTRACT Unclassified	c. THIS PAGE Unclassified	UU	22
<b>19b. TELEPHONE NUMBER (Include area code)</b> (301) 394-4627				

Standard Form 298 (Rev. 8/98)  
Prescribed by ANSI Std. Z39.18

---

## **Contents**

---

<b>List of Figures</b>	<b>iv</b>
<b>1. Introduction</b>	<b>1</b>
<b>2. Experimental Details</b>	<b>2</b>
<b>3. Results and Discussion</b>	<b>4</b>
<b>4. Conclusion</b>	<b>10</b>
<b>5. References</b>	<b>11</b>
<b>List of Symbols, Abbreviations, and Acronyms</b>	<b>13</b>
<b>Distribution List</b>	<b>15</b>

---

## List of Figures

---

Figure 1. Experimental procedure for the nano catalyst formation on the SiGe surface.....	3
Figure 2. Etch rate of $\text{Si}_{1-x}\text{Ge}_x$ in $\text{HF:H}_2\text{O}_2:\text{CH}_3\text{COOH}$ (1:2:3). .....	4
Figure 3. Pictures of AFM roughness measurements for sample (a) $\text{Si}_{0.85}\text{Ge}_{0.15}$ , (b) $\text{Si}_{0.70}\text{Ge}_{0.30}$ , and (c) $\text{Si}_{0.50}\text{Ge}_{0.50}$ . ....	5
Figure 4. %R of unetched and etched (a) $\text{Si}_{0.85}\text{Ge}_{0.15}$ , (b) $\text{Si}_{0.70}\text{Ge}_{0.30}$ , and (c) $\text{Si}_{0.50}\text{Ge}_{0.50}$ .....	6
Figure 5. Absorbance of thinned $\text{Si}_{1-x}\text{Ge}_x$ samples after lapping and polishing. ....	7
Figure 6. Absorbance spectrum of etched and unetched samples of (a) $\text{Si}_{0.85}\text{Ge}_{0.15}$ , (b) $\text{Si}_{0.70}\text{Ge}_{0.30}$ , and (c) $\text{Si}_{0.50}\text{Ge}_{0.50}$ . ....	8
Figure 7. The surface texture pattern of the sample $\text{Si}_{0.85}\text{Ge}_{0.15}$ . ....	9
Figure 8. The surface texture pattern of the sample $\text{Si}_{0.70}\text{Ge}_{0.30}$ . ....	9
Figure 9. The surface texture pattern of the sample $\text{Si}_{0.50}\text{Ge}_{0.50}$ . ....	10

---

## 1. Introduction

---

Over the past 10 years, new phenomena based on nanostructuring the surface of silicon (Si) have been investigated for application to infrared imaging. In 2003, Mazur and colleagues reported that using femtosecond laser processing coupled with halogenated etching gas, silicon surfaces having sub-micrometer corrugated conical tip microstructures could be produced (1). These microstructures had the special property that the surface of the silicon was rendered almost perfectly non-reflective. They named this material “black silicon.” In that early study, they showed that when they produced that microstructure using only halogenated etching gas (sulfur hexafluoride [SF<sub>6</sub>]) the spectral absorbance of light was extended well beyond that which would be expected from conventional band-theory understanding of silicon. In subsequent reports from researchers in the Mazur group, evidence began to point to the very highly doped surface region (sulfur-doped) on the etched surface that seemed to promote sub-bandgap absorption (2). In that work, they showed the important result that after forming the etched surface, the extended wavelength infrared absorbance could be decreased and almost completely eliminated because of dopant evaporation during high-temperature annealing.

Based on these early results, the Mazur Group partnered with device researchers at the University of Virginia and the University of Texas at Austin to demonstrate a novel infrared detector based on this new material (3).

The researchers in this partnership showed two very important demonstrations: (1) the spectral responsivity was enhanced compared to that of conventional silicon photodetectors and (2) responsivity was obtained at longer infrared wavelengths (1.3 and 1.55 μm), beyond the spectral range generally expected from silicon, which is limited to about 0.85 μm. While there is some uncertainty about the mechanism that enables sub-bandgap, longer wavelength detection, the mechanism is currently explained as longer wavelength photons excite carriers across the energy difference between mid-gap defect states from the heavily doped region and the conduction band edge. While the science behind the phenomena is being resolved, these interesting results presage new, low-cost near-infrared detectors that could have important military and civilian applications. However, for tactical military applications, a much higher spectral response at extended wavelengths in the near-infrared (~2 μm) would be desired. To that end, we are investigating silicon-germanium (Si<sub>1-x</sub>Ge<sub>x</sub>) materials with the goal of obtaining an improved photo response out to 2 μm by (1) shrinking the bandgap so that the *difference between the conduction band-edge and the defect state is reduced* and (2) providing a naturally larger absorption coefficient for longer wavelength light. So this work builds upon the results reported from the Mazur and partner groups and investigates new heavily doped black Si<sub>1-x</sub>Ge<sub>x</sub> materials. Some important differences between this work and the approach of the Mazur and partner groups are (1) we employ a metal-masked, wet-chemical etching approach versus a femtosecond gas-

phase etching process and (2) we used in-situ boron doping  $p \approx 5 \times 10^{19}/\text{cm}^3$  versus sulfur doping  $n \approx 5 \times 10^{20}/\text{cm}^3$  from the past work.

Our investigation with black  $\text{Si}_{1-x}\text{Ge}_x$  is very important since SiGe is a good substitute material for Si for many applications in low-power and high-speed semiconductor device technologies (4, 5). It is a promising material for quantum well devices (6), infrared detectors (7), and modulation doped field-effect transistors (MODFET) (8, 9). Recently, much work has been planned to use  $\text{Si}_{1-x}\text{Ge}_x$  for optodetectors and micro-electro-mechanical systems (MEMS) sensors and actuators. Activity is also being continued to develop flip chip optical receives. Among the many other applications currently being considered are strained SiGe on silicon to be used as base in a heterojunction bipolar transistor (HBT) in a bipolar complementary metal oxide semiconductor (BiCMOS) process and complementary metal oxide semiconductor (CMOS) logic applications. SiGe has much to offer for the fabrication of devices with improved efficiency (10). In a particular instance, self assembled Ge-islands and black Ge based on nano-needle arrays have been developed (11).

Increased absorption of light is essential to create highly efficient opto-sensors and photovoltaic devices. To achieve this, efficient three-dimensional (3-D) structures with relevant material systems are required. Apart from these two techniques, others (12, 13) have proposed a technique in which multicrystalline SiGe bulk crystal with microscopic compositional distribution is grown using the casting technique. The average Ge composition was changed systematically between 0% and 10%. A small addition of Ge to multicrystalline Si was found to be very effective to increase the short-circuit current density without affecting open circuit voltage. They also indicated that such grown SiGe materials are promising candidates for solar cell and other opto-electronic applications. For such applications, SiGe has to be prepared with reduced reflectivity and increased absorbance. This can be achieved through surface texturing, as has been used in the case of black silicon. In general, for a 3-D blackened surface, reactive ion etching or wet anisotropic etching are the techniques of choice. Although reactive ion etching can provide a structure with a high aspect ratio, it involves rather complicated procedures. Metal enhanced etching (MEE) (14, 15), by which silicon is etched using metal thin films or particle as catalysts, is an attractive procedure because it is simple and easier to perform with good results.

---

## 2. Experimental Details

---

The SiGe layers in this work were grown on 8-in high-resistance (111) silicon substrates using a special ultra-high vacuum chemical vapor deposition (UHV-CVD) reactor. Three planar SiGe alloys were prepared:  $\text{Si}_{0.50}\text{Ge}_{0.50}$ ,  $\text{Si}_{0.70}\text{Ge}_{0.30}$ , and  $\text{Si}_{0.85}\text{Ge}_{0.15}$ . The thickness of all SiGe layers was about  $1.25 \mu\text{m}$ . Using such a large thickness assures that although some small residual strain probably exists after growth, the large misfit strain is mostly relaxed through the introduction of dislocations. In order to avoid strain induced surface undulations in such highly compressively

strained layers, the SiGe were grown at 350–400 °C. Although UHV-CVD growth allows highly perfect crystalline quality with little impurity incorporation even with growth rates as low as  $10^{-3}$  Å/s, we have intentionally doped all layers of this study to achieve near-degenerate p-type doping. Hall effect characterization yielded the typical result that  $p = 3.47 \times 10^{20}/\text{cm}^3$ . The Seebeck coefficient was determined to be  $28 \times 10^{-6}$  V/K and is consistent with the near-degenerate doping level. There was some variation in the measured Hall mobility, but the range was always  $< 100 \text{ cm}^2/\text{V}\cdot\text{s}$  because of alloy-scattering and scattering from dislocations and ionized impurities. In this experiment, test samples mole fractions of 0.15, 0.30, and 0.50 Ge were used. Cleaned samples were used for atomic force microscopy (AFM), and the spectroscopic percent reflection (%R) and percent transmission (%T) measurements. Another set of samples were cleaned and loaded into the e-beam evaporator. The pressure in the evaporator was maintained below  $1 \times 10^{-6}$  mTorr gold (Au) was evaporated of at a rate  $0.1 \text{ \AA}$  per second to attain a thickness of  $20 \text{ \AA}$ . The samples were then annealed in a rapid thermal annealing (RTA) system for 30 min at 500 °C with argon (Ar) gas flow. These steps are shown in figure 1.

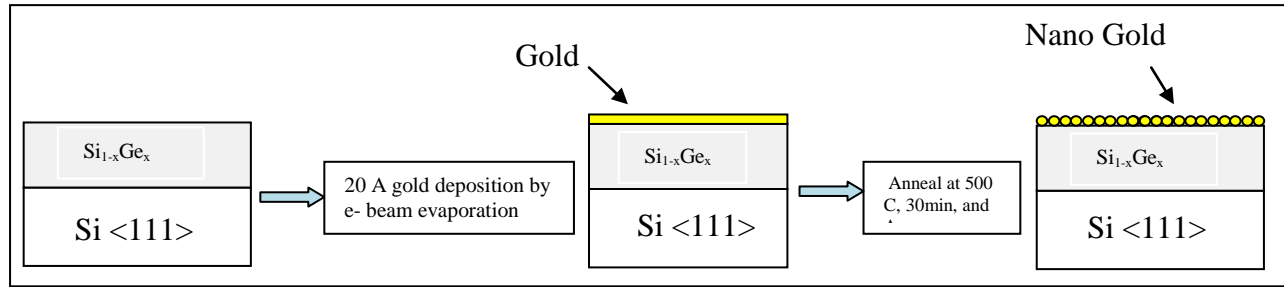


Figure 1. Experimental procedure for the nano catalyst formation on the SiGe surface.

The samples were inspected using AFM to make sure nanoparticles of Au are randomly oriented on the surface of  $\text{Si}_{1-x}\text{Ge}_x$ . In the next part of the experiment, a set of samples without Au were etched in solution of  $\text{HF:H}_2\text{O}_2:\text{CH}_3\text{COOH}$  (1:2:3) with masking to find the etch rate. Care was taken to wait 30 min prior to using this etchant. The etching of the samples in the above solution showed linearity in the etch rate and proceeded to darkened surface. Once the etch rate was determined for different compositions of  $\text{Si}_{1-x}\text{Ge}_x$ , etching was carried out with a newly prepared solution of  $\text{HF:H}_2\text{O}_2:\text{CH}_3\text{COOH}$  (1:2:3) without additional masking. After etching in that solution as part of the texturing process, the samples were thoroughly cleaned and blowdried with nitrogen. The solution etched  $\text{Si}_{1-x}\text{Ge}_x$  while slowly preserving the surface polish. However, etching the samples for more than 10 min showed visible damage. Finally, the etched samples were dipped in an aqueous solution of iodine (I) and potassium iodide (KI) (25 gm I and 100 gm KI per liter of water [ $\text{H}_2\text{O}$ ]) (16). The samples were further cleaned in running de-ionized water and dried with nitrogen. These samples were further used for AFM surface analysis and optical reflection and transmission measurements using a Perkin Elmer 950 UV-Visible-Near IR spectrometer.

### 3. Results and Discussion

All the samples were cleaned and surface characterized using AFM prior to the experiment. Some of the samples were thinned by lapping and polishing using a Logitech 10 System. Here the goal was to make sure that the samples under consideration were double-side polished to reduce the specular reflections. Samples were cleaned, and 20 Å of Au was deposited on the  $\text{Si}_{1-x}\text{Ge}_x$  surface in an e-beam evaporator, which was kept at a pressure lower than  $1 \times 10^{-6}$  mTorr. Small pieces of these samples with appropriate masking were etched with HF:H<sub>2</sub>O<sub>2</sub>:CH<sub>3</sub>COOH (1:2:3), which was freshly prepared and left at room temperature for 30 min for stabilization before use. Etching was done at room temperature (25 °C) in polypropylene beakers with slight agitation. The samples were 1 cm<sup>2</sup> in area in area in ~100 ml of fresh solution of HF:H<sub>2</sub>O<sub>2</sub>:CH<sub>3</sub>COOH (1:2:3). Figure 2 shows the etching behavior of  $\text{Si}_{1-x}\text{Ge}_x$  in HF:H<sub>2</sub>O<sub>2</sub>:CH<sub>3</sub>COOH (1:2:3).

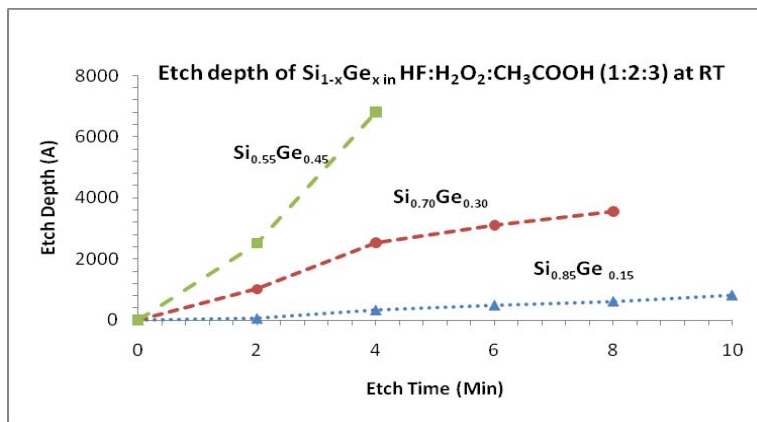


Figure 2. Etch rate of  $\text{Si}_{1-x}\text{Ge}_x$  in HF:H<sub>2</sub>O<sub>2</sub>:CH<sub>3</sub>COOH (1:2:3).

The linear etching behavior is clearly evident from the Ge concentration in the  $\text{Si}_{1-x}\text{Ge}_x$ . The rapid increase in etch rate can be explained by the presence of an increased number of Ge surface atoms. The bonding energy reveals the difficulty in breaking the Si-Si bonds (compared to Ge-Si and Ge-Ge bonds) is 78 kcal/mol; the Ge-Si bond dissociation energy is 72 kcal/mol and the Ge-Ge bond dissociation energy is 65 kcal/mol (17). The more Ge-Ge and Ge-Si bonds are exposed, the higher the etching rate is, as can be seen from the graph. The etched surface provided a greyish blackened surface.

The goal of finding the reduction in reflectivity and an increase in absorption was pursued as the next step. Etched and non-etched samples of size 1 by 1 cm were used for the optical measurements. Samples were cleaned with acetone and isopropyl alcohol (IPA), followed by blow drying with nitrogen. The samples after thermal annealing were used for optical and AFM surface measurements. The AFM scanned surface plot is given in two cases in figure 3.

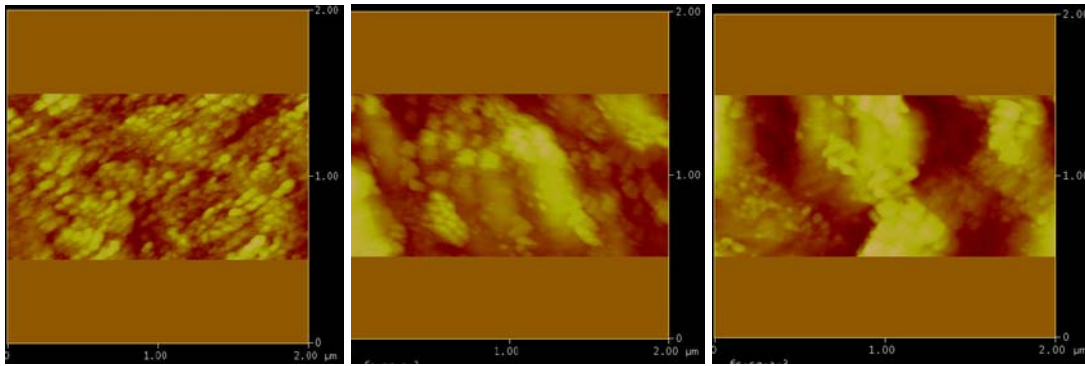


Figure 3. Pictures of AFM roughness measurements for sample (a)  $\text{Si}_{0.85}\text{Ge}_{0.15}$ , (b)  $\text{Si}_{0.70}\text{Ge}_{0.30}$ , and (c)  $\text{Si}_{0.50}\text{Ge}_{0.50}$ .

The scanned area was 2  $\mu\text{m}$  and the root mean squared (rms) values obtained in all three cases were as follows: sample 1 ( $\text{Si}_{0.85}\text{Ge}_{0.15}$ )  $\sim 37-18 \text{ nm}$ , sample 2 ( $\text{Si}_{0.70}\text{Ge}_{0.30}$ )  $\sim 40.94 \text{ nm}$ , and sample 3 ( $\text{Si}_{0.50}\text{Ge}_{0.50}$ )  $\sim 203.9 \text{ nm}$ . Clearly, the rms value increases as the amount of Ge increases; the sample numbers from 1 to 3 clearly indicate the nature of the surface. Since the contour of the Au nanoparticle surface mimics the real surface, it certainly indicates the progressive nature of the roughness as the amount of Ge increases in the sample.

Optical measurements were performed as follows. After measuring the %T and %R, we used the equation,  $A = 1 - T - R$ , to obtain the absorbance. Unetched, etched, thinned, and annealed samples were used for the measurement of %T and %R, which we then applied to the above formula to calculate the percent absorbance. The results etched and unetched samples are plotted in figure 4. The spectrum shows the reflectivity behavior of a thin film—the thickness being  $\sim 1.6 \mu\text{m}$  of the  $\text{Si}_{1-x}\text{Ge}_x$  layer on the Si (111) substrate.

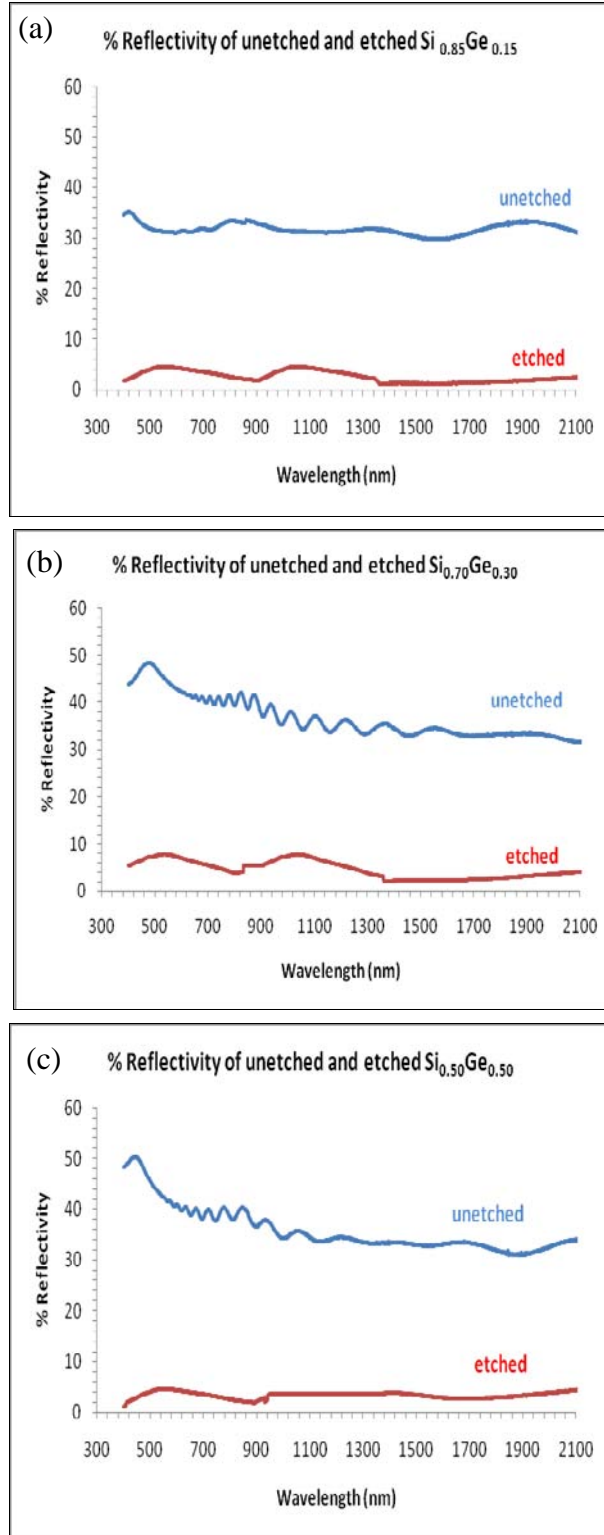


Figure 4. %R of unetched and etched (a)  $\text{Si}_{0.85}\text{Ge}_{0.15}$ ,  
(b)  $\text{Si}_{0.70}\text{Ge}_{0.30}$ , and (c)  $\text{Si}_{0.50}\text{Ge}_{0.50}$ .

The spectrum shows considerable reduction in reflectivity for  $\text{Si}_{1-x}\text{Ge}_x$  samples after etching, as can be seen in figure 4.

As can be observed from the plots, the reflectivity goes through substantial reduction after the etching. The reflectivity reduces by ~85% for samples by MEE especially in the IR region. This lowering of reflectivity is a definite indication of surface modification with micro-structure formation due to the wet etch processing.

Nano texturing of a surface depends on a number of factors, including the nature and constituent of the etchant, time of etching, and the metal catalyst. In many other cases when etching silicon, catalysts such as Ag, palladium (Pd), copper (Cu), and platinum (Pt) have given good results. This current work is the first time a metal enhanced wet etching was attempted with HF:H<sub>2</sub>O<sub>2</sub>:CH<sub>3</sub>COOH (1:2:3) as the etching solution for nano texturing of Si<sub>1-x</sub>Ge<sub>x</sub>. The observed optical effects can be explained by the formation of nanoscale textures on the Si<sub>1-x</sub>Ge<sub>x</sub> surface, representing an effective medium with a smooth transition of the refractive index from air to SiGe (18). In another experiment, as indicated earlier, samples were thinned by lapping and polished to make the reflection losses minimum. Such thinning and polishing lets the wafer to be double-side polished, thus minimizing reflection losses. Using the thinned samples, %R and %T were measured to calculate absorbance and the absorbance values are plotted in figure 5.

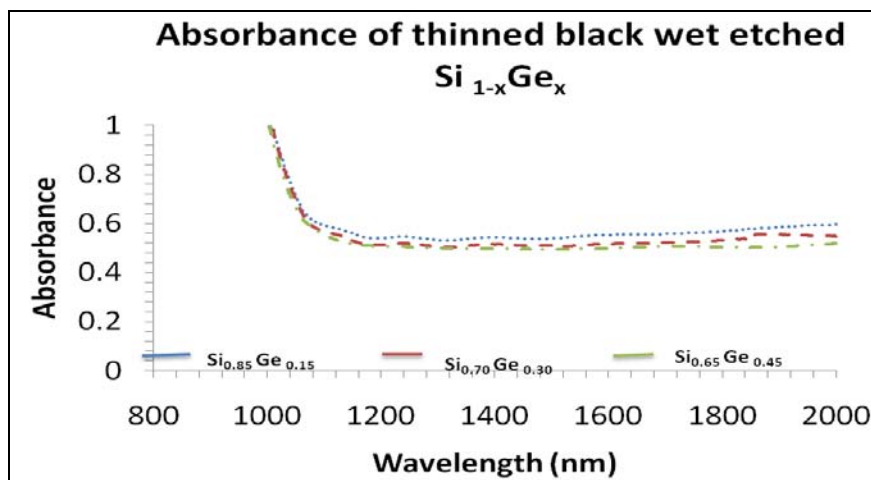


Figure 5. Absorbance of thinned Si<sub>1-x</sub>Ge<sub>x</sub> samples after lapping and polishing.

The un-thinned Si<sub>1-x</sub>Ge<sub>x</sub> samples were used for wet etching, as indicated earlier, using the etchant HF:H<sub>2</sub>O<sub>2</sub>:CH<sub>3</sub>COOH (1:2:3). The etchant was prepared and left at room temperature for ~30 min and the previously cleaned samples with Au nanoparticles were submerged for various times. To obtain appreciable darkness on the surface of samples, etching was done for about 15 min.

Samples were retrieved and cleaned in running de-ionized H<sub>2</sub>O to remove all the acid from the surface. This was followed by dipping in a solution containing KI-I<sub>2</sub> complex commercially available as Gold Etchant TFA/GE-8148 from Transene, Inc (20). This step was followed by cleaning the samples in running de-ionized H<sub>2</sub>O for 5 min, followed by blow drying them using nitrogen. These samples were used for optical characterization to obtain %T and %R.

Absorbance was calculated using the equation A = 1 - T - R. The absorbance versus the

wavelength is plotted in figure 6. The plots include the absorbance for the unetched and etched samples in each case. In all three cases, one can see that the absorbance went up, indicating the reflectivity decreased even though the %T remained the same.

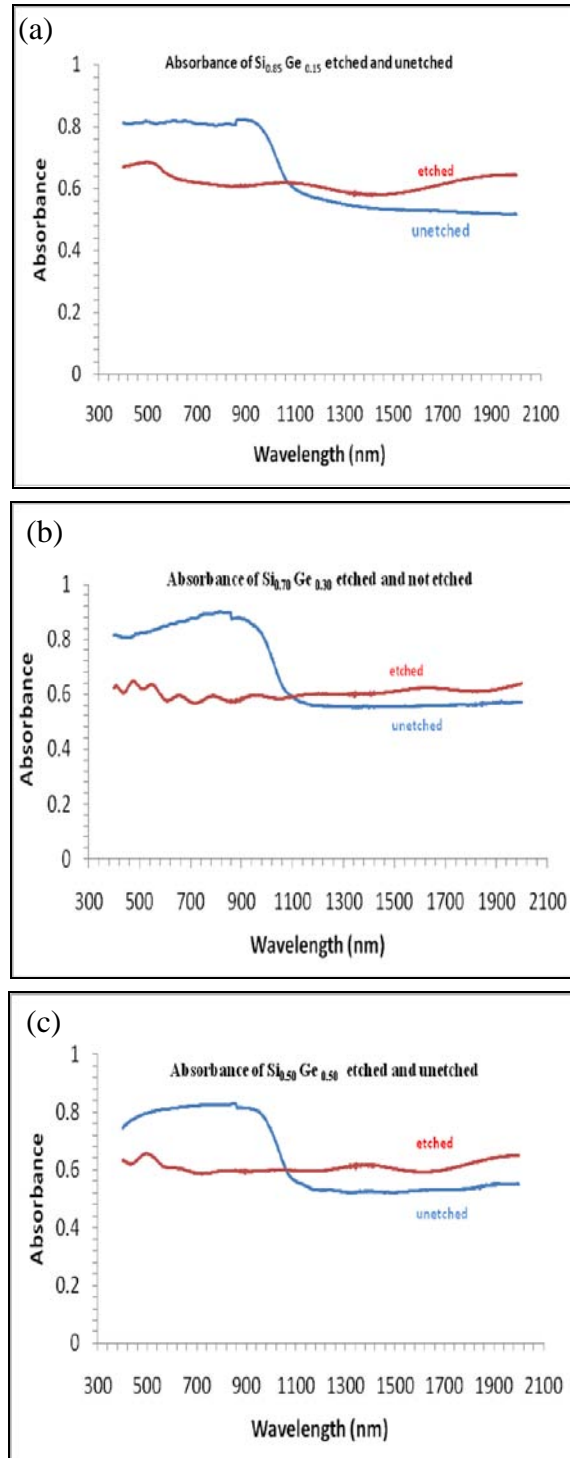


Figure 6. Absorbance spectrum of etched and unetched samples of  
 (a)  $\text{Si}_{0.85}\text{Ge}_{0.15}$ , (b)  $\text{Si}_{0.70}\text{Ge}_{0.30}$ , and (c)  $\text{Si}_{0.50}\text{Ge}_{0.50}$ .

In general, the absorbance increase is from 5–10%, the larger increase being in  $\text{Si}_{0.85}\text{Ge}_{0.15}$ . The etched samples were further characterized using a Veeco surface topography profiler. The system's white light interferometry can measure surface topography from nanometer-scale roughness through millimeter-scale steps, with a sub-nanometer resolution. This surface metrology system was used to understand the surface texture patterns and parameters of the etched surface. Figure 7 gives the surface texture pattern of the sample  $\text{Si}_{0.85}\text{Ge}_{0.15}$ . The curves on the right indicate the  $x$ -axis (red) and  $y$ -axis (blue), as indicated on the middle cross wire.

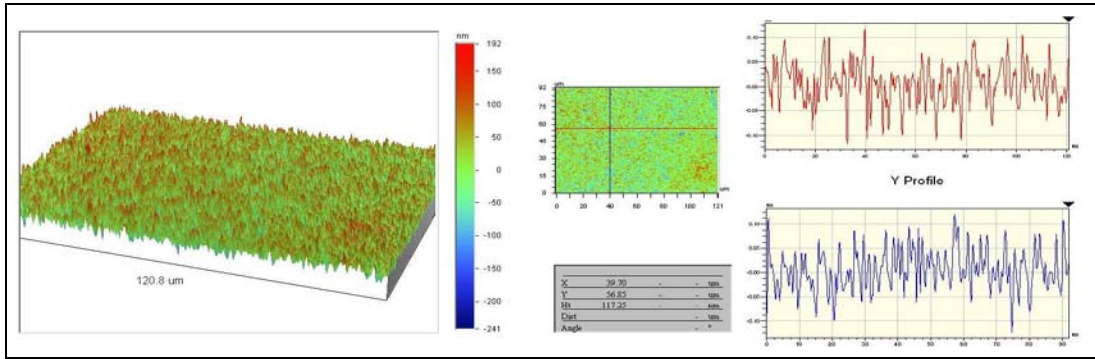


Figure 7. The surface texture pattern of the sample  $\text{Si}_{0.85}\text{Ge}_{0.15}$ .

Figures 8 and 9 give the surface texture pattern of  $\text{Si}_{0.70}\text{Ge}_{0.30}$  and  $\text{Si}_{0.50}\text{Ge}_{0.50}$ , respectively. Texturing is prominent in the third sample and sample  $\text{Si}_{0.50}\text{Ge}_{0.50}$  and, correspondingly, the rms value is higher as well. In figure 9, one can see more damage and separation of regions in  $\text{Si}_{1-x}\text{Ge}_x$  due to wet etching.

There may be also formations of clustered Ge regions on the surface. This argument can be justified by the  $x$ - $y$  plot on the right side in figure 9, unlike in figure 7 and 8, where the  $x$ - $y$  plots are spaced closely.

One of the reasons for this behavior is the presence of a lower amount of Si in  $\text{Si}_{1-x}\text{Ge}_x$  and a higher amount of Ge.

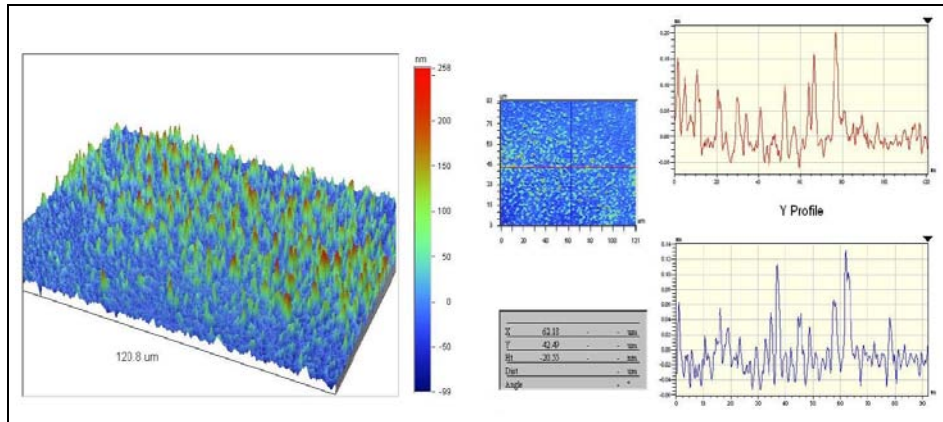


Figure 8. The surface texture pattern of the sample  $\text{Si}_{0.70}\text{Ge}_{0.30}$ .

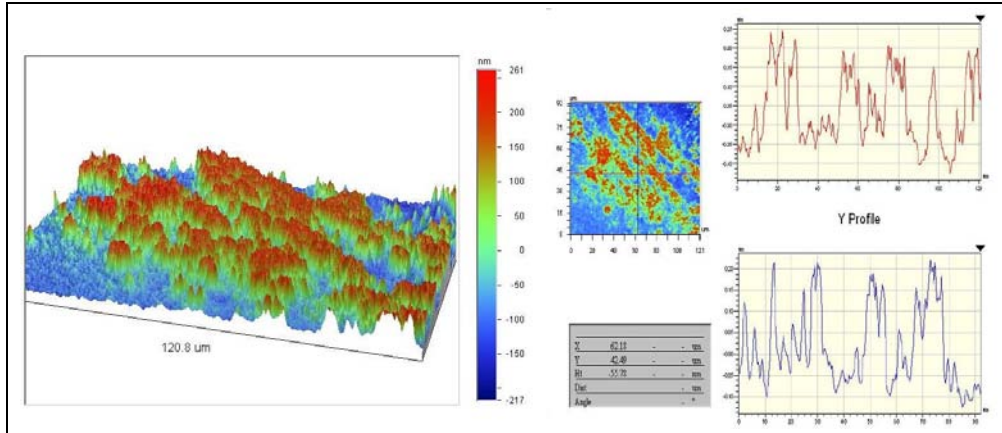


Figure 9. The surface texture pattern of the sample  $\text{Si}_{0.50}\text{Ge}_{0.50}$ .

#### 4. Conclusion

We reported here for the first time an investigation of optical properties of reflection and absorbance of compositional  $\text{Si}_{1-x}\text{Ge}_x$  semiconductor alloys after treating with metal enhanced chemical etching using nano-sized Au particles as the catalyst and  $\text{HF:H}_2\text{O}_2:\text{CH}_3\text{COOH}$  as the etchant. The etched surface became black, textured, and showed a suppression of reflectivity and an enhancement of absorption in the near-infrared region. Conceivably, the black  $\text{Si}_{1-x}\text{Ge}_x$  became micro-structured due to the metal catalysis and wet etching. Surface texturing was visible, as shown by the plots, and became extreme in the case of  $\text{Si}_{0.55}\text{Ge}_{0.45}$ . Visible separation in the  $x$ - $y$  plots positively indicates this behavior, which is due to the lower amount of Si and an excess amount of Ge in  $\text{Si}_{1-x}\text{Ge}_x$ . Through this work, we have shown that  $\text{Si}_{1-x}\text{Ge}_x$  can be made black using metal enhanced chemical etching. We have also shown that such black  $\text{Si}_{1-x}\text{Ge}_x$  has reduced reflectivity and enhanced absorbance in the near-infrared region.

Detectors made with this type of black  $\text{Si}_{1-x}\text{Ge}_x$  will have higher performance in the extended IR region. This lowering of reflection and enhancement of absorption may have important practical implications for making efficient photovoltaic and photodetecting applications using compositional  $\text{Si}_{1-x}\text{Ge}_x$  alloys. Currently, we are fabricating photodetectors to prove our conclusion.

---

## 5. References

---

1. Younkin, R.; Carey, J.; Mazur, E.; Levinson, J.; Friend, C. *J. Appl. Phys.* **2003**, *93* (5), 2626.
2. Crouch, C.; Carey, J.; Shen, M.; Mazur, E.; Genin, F. *Appl. Phys A* **2004**, *79*, 1635.
3. Huang, Z.; Carey, J.; Liu, M.; Guo, X.; Mazur, E.; Campbell, J. *Appl. Phys. Lett.* **2006**, *89*, 033506.
4. Konig, U.; Gruhle, A. *Proceedings of the 1997 IEEE/Cornell Conference on Advanced Concepts in High Speed Semiconductor Devices and Circuits*, IEEE, Ithaca, NY, 1997.
5. Grimmeiss, H. G. *Semiconductors* **1999**, *33*, 939.
6. Nayak, D. K.; Woo, J. C.; Park, J. S.; Wang, K. L.; MacWilliams, K. P. *IEEE Electron Device Lett. EDL-12-154* **1991**.
7. Luryi, S.; Kastalsky, A.; Bean, J. C. *IEEE Trans. Electron Devices ED-31* **1984**, *1135*.
8. Perasall, T. P.; Bean, J. C. *IEEE Electron Device Lett. EDL-7* **1986**, *308*.
9. Venkataraman, V.; Liu, C. W.; Strum, J. C. *J. Vac. Sci. Technol* **1993**, *B 11*, 1176.
10. Williamson, D. L. *Solar Energy Materials and Solar Cells* **2003**, *78* (1–4), 41–84.
11. Chueh, Y. L.; Fan, Z.; Takei, K.; Ko, H.; Kapadia, R.; Rathore, A. A.; Miller, N.; Yu, K.; Wu, M.; Haller, E. E.; Javey, A. *Nano Lett.* **2010**, *10*, 520.
12. Koynov, S.; Brandt, M. S.; Stutzmann, M. *App. Phys. Lett.* **2006**, *88*, 203107.
13. Wu, C.; Crouch, C. H.; Zhao, L.; Carey, J. E.; Yonkin, R.; Levinson, J. A.; Mazur, E.; Farrell, R. M.; Gothoskar, P.; Karger, A. *App. Phys. Lett.* **2001**, *73*, 1850.
14. Nakajima, K.; Usami, N.; Fujiwara, K.; Murakami, Y.; Ujihara, T.; Sazaki, G.; Shishido, T. *Sol. Energy Mater. Sol. Cells* **2002**, *72*, 93.
15. Nakajima, K.; Usami, N.; Fujiwara, K.; Murakami, Y.; Ujihara, T.; Sazaki, G.; Shishido, T. *Sol. Energy Mater. Sol. Cells* **2002**, *73*, 305.
16. Li, X.; Boh, P. W. *Appl. Phys. Lett.* **2000**, *77*, 2572.
17. Yee, S.; Kawamoto, Y.; Tanaka, H.; Fukumuro, N.; Matsuda, H. *Elechem. Comm.* **2003**, *5*, 632.
18. Schumb, W. C.; Satterfield, C. N.; Wentworth, R. L. in *Hydrogen Peroxide*, Reinhold Publishing, New York, 1955, p. 370.

19. Kishioka, K.; Horita, S.; Ohdaria, K.; Matsumura, H. *Sol. Energy Mater. Sol. Cells* **2008**, 92, 919.
20. Transene Company Web page. [http://www.transene.com/au\\_etchant.html](http://www.transene.com/au_etchant.html) (accessed 2010).

---

## List of Symbols, Abbreviations, and Acronyms

---

%R	percent reflection
%T	percent transmission
3-D	three-dimensional
AFM	atomic force microscopy
Ar	argon
Au	gold
BiCMOS	bipolar complementary metal oxide semiconductor
CMOS	complementary metal oxide semiconductor
Cu	copper
Ge	germanium
H <sub>2</sub> O	water
HBT	heterojunction bipolar transistor
I	iodine
IPA	isopropal alcohol
KI	potassium iodide
MEE	metal enhanced etching
MEMS	micro-electro-mechanical systems
MODFET	modulation doped field-effect transistors
Pd	palladium
Pt	platinum
rms	root mean squared
RTA	rapid thermal annealing
SF <sub>6</sub>	sulfur hexafluoride
Si	silicon

$\text{Si}_{1-x}\text{Ge}_x$  silicon-germanium

UHV-CVD ultra-high vacuum chemical vapor deposition

NO. OF COPIES	ORGANIZATION	NO. OF COPIES	ORGANIZATION
1 ELECT	ADMNSTR DEFNS TECHL INFO CTR ATTN DTIC OCP 8725 JOHN J KINGMAN RD STE 0944 FT BELVOIR VA 22060-6218	1	US GOVERNMENT PRINT OFF DEPOSITORY RECEIVING SECTION ATTN MAIL STOP IDAD J TATE 732 NORTH CAPITOL ST NW WASHINGTON DC 20402
1	DARPA MTO ATTN N DHAR 3701 NORTH FAIRFAX DR ARLINGTON VA 22203-1714	1	GENERAL TECHNICAL SERVICES ATTN G P MEISSNER 3100 ROUTE 138 WALL NJ 07719
1 CD	OFC OF THE SECY OF DEFNS ATTN ODDRE (R&AT) THE PENTAGON WASHINGTON DC 20301-3080	1	US ARMY RSRCH LAB ATTN RDRL CIM G T LANDFRIED BLDG 4600 ABERDEEN PROVING GROUND MD 21005-5066
1	US ARMY RSRCH DEV AND ENGRG CMND ARMAMENT RSRCH DEV & ENGRG CTR ARMAMENT ENGRG & TECHNLGY CTR ATTN AMSRD AAR AEF T J MATTS BLDG 305 ABERDEEN PROVING GROUND MD 21005-5001	1	DIRECTOR US ARMY RSRCH LAB ATTN RDRL ROE L W CLARK PO BOX 12211 RESEARCH TRIANGLE PARK NC 27709
2	CECOM NVESD ATTN AMSEL RD NV A SCHOLTZ ATTN AMSEL RD NV D BENSON 10221 BURBECK RD STE 430 FT BELVOIR VA 22060-5806	58	ARMY RSRCH LAB ATTN IMNE ALC HRR MAIL & RECORDS MGMT ATTN RDRL CIM L TECHL LIB ATTN RDRL CIM P TECHL PUB ATTN RDRL SE J PELLEGRINO ATTN RDRL SE E L BLISS ATTN RDRL SE E T BOWER ATTN RDRL SED E M LITZ ATTN RDRL SED P A LELIS ATTN RDRL SED P B MORGAN ATTN RDRL SED P K JONES ATTN RDRL SEE G WOOD ATTN RDRL SEE P GILLESPIE ATTN RDRL SEE E T ALEXANDER ATTN RDRL SEE E K ALIBERTI ATTN RDRL SEE E N GUPTA ATTN RDRL SEE E R TOBER ATTN RDRL SEE I S TRIVEDI ATTN RDRL SEE I B ZANDI ATTN RDRL SEE I D BEEKMAN ATTN RDRL SEE I F SEMENDY (5 COPIES) ATTN RDRL SEE I G BRILL ATTN RDRL SEE I J LITTLE ATTN RDRL SEE I K K CHOI
1	PM TIMS, PROFILER (MMS-P) AN/TMQ-52 ATTN B GRIFFIES BUILDING 563 FT MONMOUTH NJ 07703		
1	US ARMY INFO SYS ENGRG CMND ATTN AMSEL IE TD A RIVERA FT HUACHUCA AZ 85613-5300		
1	COMMANDER US ARMY RDECOM ATTN AMSRD AMR W C MCCORKLE 5400 FOWLER RD REDSTONE ARSENAL AL 35898-5000		

NO. OF  
COPIES ORGANIZATION

ATTN RDRL SEE I K OLVER  
ATTN RDRL SEE I P FOLKES  
ATTN RDRL SEE I P TAYLOR  
ATTN RDRL SEE I P UPPAL  
ATTN RDRL SEE I S FARRELL  
ATTN RDRL SEE I S SVENSSON  
ATTN RDRL SEE I W BECK  
ATTN RDRL SEE I W SARNEY  
ATTN RDRL SEE I Y CHEN  
ATTN RDRL SEE M G DANG  
ATTN RDRL SEE M G GARRETT  
ATTN RDRL SEE M M REED  
ATTN RDRL SEE M  
M TAYSING-LARA  
ATTN RDRL SEE M M WRABACK  
ATTN RDRL SEE M N BAMBHA  
ATTN RDRL SEE M N DAS  
ATTN RDRL SEE M P SHEN  
ATTN RDRL SEE M W CHANG  
ATTN RDRL SEE O N FELL  
ATTN RDRL SEE O P PELLEGRINO  
ATTN RDRL SEG N MARK  
ATTN RDRL SER E A DARWISH  
ATTN RDRL SER E P SHAH  
ATTN RDRL SER L A WICKENDEN  
ATTN RDRL SER L B NICHOLS  
ATTN RDRL SER L E ZAKAR  
ATTN RDRL SER L M DUBEY  
ATTN RDRL SER L M ERVIN  
ATTN RDRL SER L S KILPATRICK  
ATTN RDRL SER P AMIRTHARAJ  
ATTN RDRL SER U C FAZI  
ADELPHI MD 20783-1197

TOTAL: 71 (69 HCS, 1 CD, 1 ELECT)